



Mapping sugarcane globally at 10 m resolution using GEDI and Sentinel-2

Stefania Di Tommaso¹, Sherrie Wang², Rob Strey³, and David B. Lobell¹

¹Department of Earth System Science & Center on Food Security and the Environment, Stanford University, USA

²Department of Mechanical Engineering & Institute for Data, Systems, and Society, MIT, USA

³Progressive Environmental & Agricultural Technologies, 10435 Berlin, Germany

Correspondence: David B. Lobell (dlobell@stanford.edu)

1 **Abstract.** Sugarcane is an important source of food, biofuel, and farmer income in many countries. At the same time, sugarcane
2 is implicated in many social and environmental challenges, including water scarcity and nutrient pollution. Currently, few of the
3 top sugar-producing countries generate reliable maps of where sugarcane is cultivated. To fill this gap, we introduce a dataset
4 of detailed sugarcane maps for the top 13 producing countries in the world, comprising nearly 90% of global production. Maps
5 were generated for the 2019-2022 period by combining data from the Global Ecosystem Dynamics Investigation (GEDI) and
6 Sentinel-2 (S2). GEDI data were used to provide training data on where tall and short crops were growing each month, while S2
7 features were used to map tall crops for all cropland pixels each month. Sugarcane was then identified by leveraging the fact that
8 sugar is typically the only tall crop growing for a substantial fraction of time during the study period. Comparisons with field
9 data, pre-existing maps, and official government statistics all indicated high precision and recall of our maps. Agreement with
10 field data at the pixel level exceeded 80% in most countries, and sub-national sugarcane areas from our maps were consistent
11 with government statistics. Exceptions appeared mainly due to problems in underlying cropland masks, or to under-reporting
12 of sugarcane area by governments. The final maps should be useful in studying the various impacts of sugarcane cultivation
13 and producing maps of related outcomes such as sugarcane yields.

14 1 Introduction

15 Sugarcane cultivation represents an important economic activity in many regions of the world, and serves as a substantial source
16 of food, beverage, and biofuel production. Roughly one-quarter of all ethanol production worldwide comes from sugarcane
17 (OECD et al., 2023), with many countries aiming to rapidly increase sugar ethanol production to meet energy independence
18 and climate mitigation goals. For example, the OECD/FAO projects that ethanol demand over the next decade will increase by
19 37% in Brazil and 107% in India (OECD et al., 2023), both countries where sugarcane is the primary feedstock. Moreover,
20 millions of livelihoods are derived from sugarcane production and processing activities, with some estimates putting the total
21 number of livelihoods dependent on sugarcane as high as 100 million (Jenkins et al., 2015).

22 Despite its contribution to food and energy security and economic growth, sugarcane cultivation has also been associated
23 with myriad challenges, including but not limited to large consumption of available freshwater and fertile cropland (Lee et al.,
24 2020), pollution of soils and ecosystems with nutrients and other chemical runoff (Allan et al., 2017), and exploitative labor



25 conditions (El Chami et al., 2020). In addition, sugarcane receives a disproportionate amount of policy support in many coun-
26 tries through mechanisms such as market price support, ethanol mandates, and assistance to sugar mills. According to recent
27 OECD estimates, sugar receives commodity-specific transfers of more than 20% of farm receipts globally, higher than any
28 other food commodity (OECD, 2023). In some countries, this share is much higher, such as Mexico (37%), the United States
29 (48%), Indonesia (55%), and the Philippines (62%) (OECD, 2023).

30 Despite the prominent role of sugarcane in many economies and the key support from government, few countries provide
31 timely information on the status and dynamics of sugar cultivation. Such information could be helpful in studying the full
32 effects of sugar cultivation on the health of both humans and the environment, thus informing public policy. Better data could
33 also help aid sugar producers in their attempts to optimize productivity and profits, for example by helping to better understand
34 factors that determine yield variation.

35 In an effort to fill the significant data gaps relating to sugarcane cultivation, we present here an approach and dataset that
36 uses satellite remote sensing to map precise locations of sugarcane canopies around the world. Remote sensing has long been
37 used to map areas of individual crops, with several countries producing annual, publicly available maps of crop types based
38 on satellite data, such as the Cropland Data Layer (CDL) in the United States (Boryan et al., 2011) and the Annual Crop
39 Inventory in Canada (Agriculture and Agri-Food Canada). Yet these maps have historically required ground data to calibrate
40 the satellite models each year, which precludes their use in countries without a concerted government effort to maintain ground
41 data collection.

42 Rather than rely on ground data, our approach relies on two features of sugarcane that together make it a unique crop
43 throughout most of the regions where it is grown – it is much taller than most crops (often exceeding 3 meters in height), and
44 grows across multiple years. In recent work (Di Tommaso et al., 2021, 2023), we demonstrated the ability of lidar measurements
45 acquired by the Global Ecosystem Dynamics Investigation (GEDI) (Dubayah et al., 2020) to identify tall canopies within
46 agricultural landscapes. Here we extend that work to map tall crops in each month over a four year period, and then identify
47 sugarcane fields as those that are tall for a sufficiently large fraction of the study period. We find that this approach is able to
48 map sugarcane with impressive detail across a wide number of countries, using both government statistics and independent
49 maps in some countries to evaluate our product.

50 **2 Datasets**

51 The datasets utilized in this study include:

- 52 1. GEDI and Sentinel-2 Sensors: Data from the Global Ecosystem Dynamics Investigation (GEDI) and Sentinel-2 (S2)
53 satellite sensors were employed for data acquisition. Pre-processing steps were taken to prepare these datasets for analysis.
- 54 2. Land Cover Products: Various land cover products were employed to delineate the cropped areas within the study area.
- 55 3. Calibration and Validation Datasets: Specific datasets were utilized for the calibration and validation of the sugarcane
56 maps generated in this study.



57 2.1 GEDI data

58 GEDI, a sensor mounted on the International Space Station (ISS), captures lidar waveforms within the latitudinal range of 51.6°
59 N to 51.6° S to analyze the Earth's surface in three dimensions. It is the first spaceborne lidar instrument specifically designed
60 for assessing vegetation structure (Dubayah et al., 2020). Equipped with three lasers emitting near-infrared light at 1064 nm
61 wavelength, GEDI features two full-power lasers along with a third laser divided into dual beams, generating a total of four
62 beams. Through optical dithering across-track, each beam creates eight ground tracks (comprising four full-power tracks and
63 four cover tracks) spaced 600 meters apart on the ground. The shots produced have an average footprint diameter of 25 meters
64 and are separated by 60 meters along-track.

65 For this study, we used the GEDI dataset Level 2A (L2A) and Level 2B (L2B) from April 2019 to December 2022, available
66 in GEE data catalog.

67 The Level 2 data offer insights into the vertical canopy distribution derived from waveform returns at the footprint level. Our
68 primary dataset was GEDI's L2A Geolocated Elevation and Height Metrics Product, primarily comprising Relative Height
69 (RH) metrics. These RH metrics collectively characterize the waveform data acquired by GEDI, providing information about
70 the height at which a specific percentage of energy is returned relative to the ground. RH values are reported at 1% intervals,
71 resulting in a total of 101 metrics. Additionally, we used the L2B dataset to extract the GEDI view angle at each shot location,
72 specifically using the 'local beam elevation' property. This information was used to filter out GEDI shots with a view angle
73 below 1.51 rad, to avoid classification errors, as recommended in Di Tommaso et al. (2023).

74 The GEDI L2A dataset (LARSE/GEDI/GEDI02_A_002_MONTHLY) and L2B dataset (LARSE/GEDI/GEDI02_B_002_MONTHLY)
75 represent a rasterized version of the original GEDI products, where each GEDI shot footprint is depicted by a 25-meter pixel
76 (Healey et al., 2020). This rasterization process, however, may introduce an additional geolocation error beyond the initial
77 GEDI shot error. The raster images are structured as monthly composites of individual orbits conducted during the respective
78 month (refer to Figure 1). Within these raster images, RH values, along with quality flags and metadata, are preserved as raster
79 bands.

80 2.2 Sentinel-2

81 We employed the S2 surface reflectance Harmonized collection, which is readily available in the Google Earth Engine (GEE)
82 platform. Clouds were filtered out using the S2 Cloud Probability dataset provided by SentinelHub in GEE. Utilizing this
83 dataset, we generated yearly (January to December) time series for each pixel. These time series were then utilized to compute
84 harmonic features, with an order of $n=3$ and $\omega=1$, for a combination of bands including 'NIR' (Near Infrared), 'SWIR1'
85 (Shortwave Infrared 1), 'SWIR2' (Shortwave Infrared 2), 'RDED4' (Red Edge Band 4), and 'GCVI' (Green Chlorophyll
86 Vegetation Index) (Gitelson et al., 2005). This approach, proven successful in previous studies, has demonstrated efficacy in
87 tasks related to crop type classification. GCVI is computed as

88 $GCVI = NIR/Green - 1$

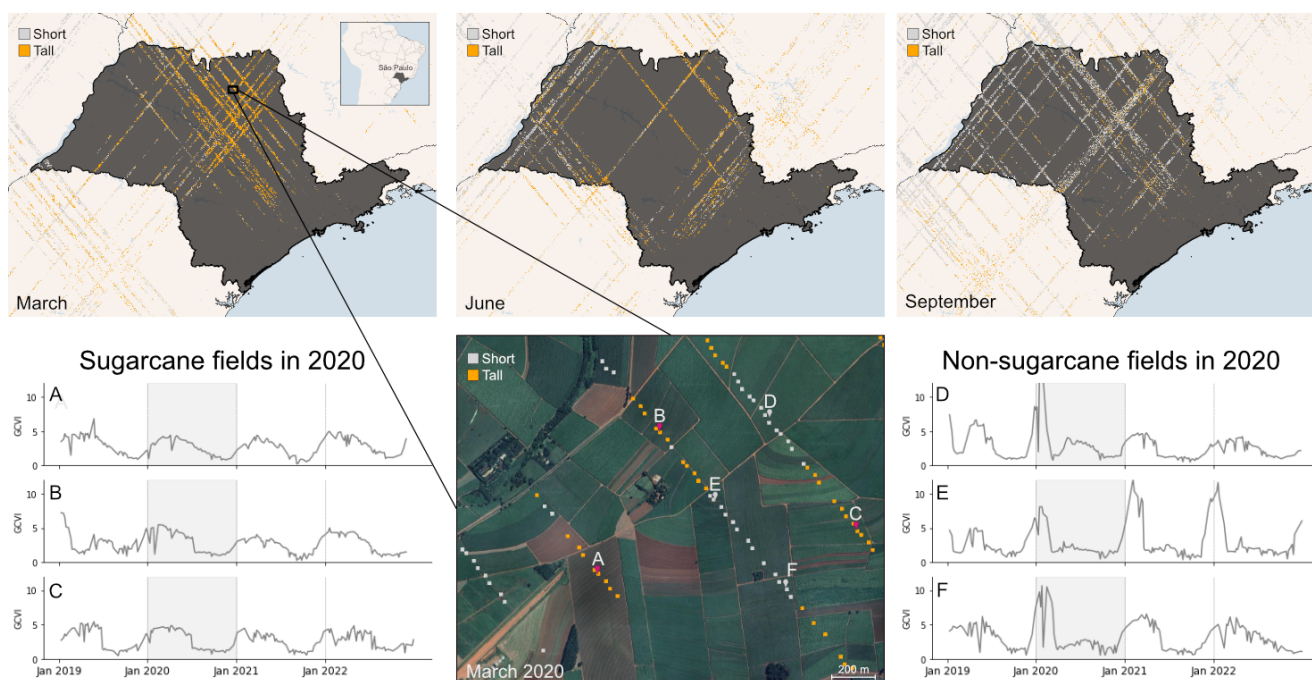


Figure 1. GEDI shots over São Paulo, the main sugarcane-producing state in Brazil. Top panel shows GEDI coverage in three different months, March, June and September, over the 4 years of data. Shots represented by a 25 m pixel are color-coded according to the short/tall classification by the GEDI model. Gaps in GEDI shot orbits may be attributed to quality issues. For instance, in June 2020, a significant portion of shots experienced low view angles and were subsequently filtered out, resulting in sparser GEDI coverage during this period, as illustrated in the top-middle panel. Additionally, in this region, there appears to be a higher proportion of shots classified as tall around the beginning of the year compared to later months. Bottom-middle panel show a zoom in at field level (© Google Earth Engine). GCVI S2 time series from 2019 to 2022 over sugarcane (on the left) and non-sugarcane fields (on the right), with the year 2020 highlighted in gray shading. GEDI accurately identifies tall fields that are growing sugarcane in March (A,B,C), and short fields that are not growing sugarcane in 2020 (D,E,F).



89 For each spectral band or vegetation index $f(t)$, the harmonic regression takes the form

$$90 \quad f(t) = c + \sum_{k=1}^n [a_k \cos(2\pi\omega kt) + b_k \sin(2\pi\omega kt)]$$

91 where a_k are cosine coefficients, b_k are sine coefficients, and c is the intercept term. The independent variable t represents
92 the time an image is taken within a year expressed as a fraction between 0 and 1. The number of harmonic terms n and the
93 periodicity of the harmonic basis controlled by ω are hyperparameters of the regression. This resulted in seven features per
94 band, for a total of 35 coefficients. These estimated values represent the S2-based harmonic features used in the subsequent
95 classification process.

96 **2.3 Crop mask**

97 Despite the abundance of global and regional cropland maps, considerable uncertainties and discrepancies persist regarding
98 both the total area and spatial distribution. To identify cropped areas comprehensively, we conducted an analysis encompassing
99 all global land cover products detailed in Kerner et al. (2023). Through visual inspection and subsequent examination of the
100 datasets outlined later, we observed that relying solely on a single product often resulted in the underestimation of cropland
101 area in certain regions, while another product exhibited similar limitations elsewhere. Recognizing the inherent risk of inac-
102 curate crop masks leading to either over- or underestimation, we opted to ensure a more robust global coverage by integrating
103 information from three distinct global land cover products. We defined a pixel as cropland if any of the three maps classified it
104 as such. This approach, involving the combination of these datasets, enabled us to enhance the completeness of cropland areas
105 worldwide.

106 The three global products are: the European Space Agency (ESA) WorldCover 2020 (Zanaga et al., 2021), ESRI 2020 global
107 Land Use Land Cover (Karra et al., 2021) and the 2019 GLAD Global Cropland Maps (Potapov et al., 2022).

108 A visual example of the three crop masks is provided for Brazil in Figure 2.

109 The ESA and ESRI 2020 products provide a global land cover map for 2020 at 10 m resolution, the former based on
110 Sentinel-1 and Sentinel-2 data, and the latter based on Sentinel-2 alone. Maps are available in the Google Earth Engine (GEE)
111 (Gorelick et al., 2017) official and community data catalogs, respectively (Roy et al., 2024). The 2019 GLAD Map provides
112 binary cropland classifications at 30 m. Classification is performed using bagged decision trees with features extracted from
113 time series of Landsat Analysis Ready Data (ARD).

114 Divergences exist among these land cover and land use products regarding the categorization of croplands, particularly
115 concerning the inclusion of tree crops. ESA WorldCover encountered issues such as underestimation of cropland areas in Brazil
116 and Africa, particularly in fragmented regions with mixed land covers. Contrarily, the WorldCover 2020 product identified more
117 tree cover, representing orchards, compared to other ESRI products.

118 ESA's definition of cropland encompasses land that is covered with annual crops sowed and harvested at least once within
119 12 months after the sowing date. This cropland typically produces an herbaceous cover and may include some tree or woody
120 vegetation but excludes perennial woody crops. ESRI defines croplands as human-planted cereals, grasses, and crops not at tree

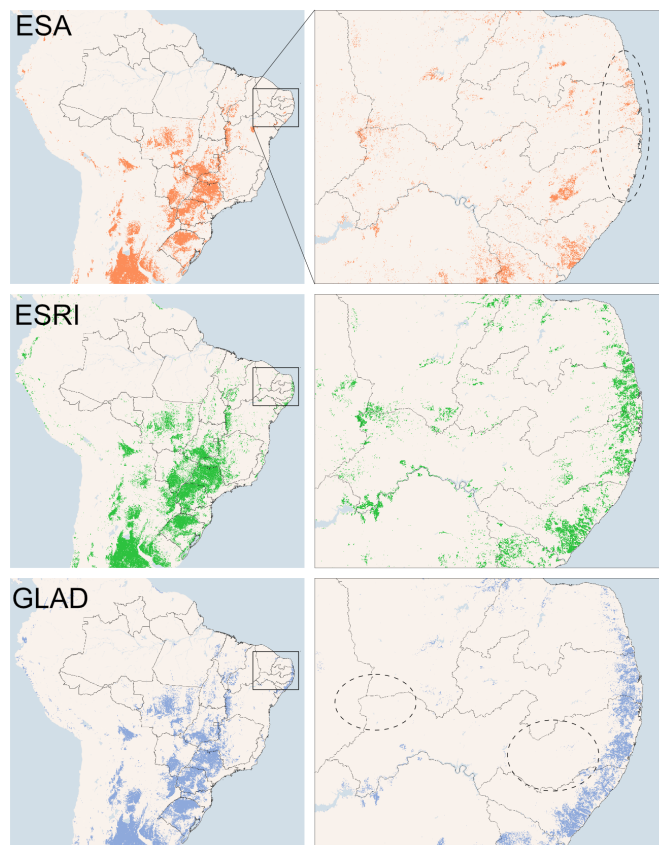


Figure 2. An example of difference in crop masks in Brazil (© Google Earth Engine). Dotted circles highlight areas of disagreement between maps. The ESA crop mask exhibits omissions in cropland detection in North-Eastern Brazil, whereas ESRI and GLAD capture more cropland in this region. ESRI tends to overmap cropland, often including orchards, while GLAD exhibits a more conservative approach, albeit missing some cropland in areas where both ESA and ESRI map it.

121 height, including rice paddies and irrigated agriculture, while GLAD excludes perennial woody crops and permanent pastures
122 from its definition, focusing on herbaceous crops for human consumption, forage, and biofuel.

123 2.4 Calibration and Validation datasets

124 Below we describe the datasets used for calibrating and validating the sugarcane maps. The data pertain to the main sugarcane-
125 producing countries according to the Food and Agriculture Organization (FAO) (Food and Agriculture Organization's Statis-
126 tical Database (FAOSTAT)), as presented in Table 1. Within each section, the countries are in decreasing order of sugarcane
127 production.



Table 1. Main sugarcane-producing countries according to FAO 2022.

Rank	Area	Production (million tonnes)	Production (%)	Area harvested (million hectares)	Area harvested (%)
1	Brazil	724	37.7	9.9	37.8
2	India	439	22.9	5.2	19.8
3	China	103	5.4	1.3	5.0
4	Thailand	92	4.8	1.5	5.8
5	Pakistan	87	4.6	1.3	5.1
6	Mexico	55	2.9	0.8	3.1
7	Colombia	35	1.8	0.4	1.4
8	Indonesia	32	1.7	0.5	1.9
9	USA	31	1.6	0.4	1.4
10	Australia	28	1.5	0.3	1.3
11	Guatemala	26	1.4	0.2	0.9
12	Philippines	23	1.2	0.4	1.5
13	South Africa	17	0.9	0.3	1.0
	Rest of the world	224	11.7	3.6	13.9

128 The list includes field-level labels, raster datasets, and government-reported sugarcane area data at administrative level 2 or
129 3. The specific sources for these datasets may vary depending on the region and the year of data collection. A summary of all
130 data available by region is provided in Table 2.

131 2.4.1 Point level data

132 The WorldCereal "sv_croptype_validations" dataset (Lesiv et al., 2023) includes observations of crop types in 2021 and 2022
133 at global scale along with their coordinates. This dataset was compiled and released by WorldCereal through a meticu-
134 lous process involving expert manual labeling. Utilizing an IIASA tool known as "Street Imagery validation" (accessible at
135 <https://svweb.cloud.geo-wiki.org/>), contributors were able to examine street-level images, including those from platforms like
136 Google Street View and Mapillary, and accurately identify crop types. It's important to note that this dataset is entirely distinct
137 and separate from existing maps and reference datasets, providing an independent source of valuable information for agri-
138 cultural analysis. The dataset contains labels for various crop types, including sugarcane, for several countries of interest. In
139 Brazil, sugarcane is the most prevalent crop label, accounting for 1.6k labels, followed by maize (~910) and soybean (~550).
140 In Mexico crop labels alongside sugarcane (50 labels) include maize (~40). Australia's crop distribution includes wheat (~120
141 labels) and sugarcane (~20). Meanwhile, in the Philippines, rice (~80 labels) is prevalent alongside sugarcane (~70).

142 Other countries represented in the WorldCereal dataset with a smaller number of samples include China, Colombia, India,
143 Pakistan, South Africa and Thailand.



Table 2. Summary of all available dataset by country and data type. The datasets used for calibrating our method are marked with an asterisk. WorldCereal point data refer to the years 2021-2022.

Country	Raster	Field points	Government statistics
Brazil	(binary) 2018-2019	World Cereal*	2022
India		Plantix 2020-2021* World Cereal	2019-2020
China	(binary) 2019-2020*	World Cereal	2022
Thailand		GSV points 2022* World Cereal	2022
Pakistan		World Cereal	2021-2022
Mexico		World Cereal*	2022
Colombia		World Cereal	2019
Indonesia			2021
USA	CDL 2019-2022*		2018
Australia		World Cereal*	2020-2021
Guatemala			2003
Philippines		World Cereal*	2021
South Africa	SANLC 2020*	SANLC points 2020 World Cereal	2017

144 In India we accessed crop type labels crowdsourced from farmers via Plantix, a free Android application developed by
 145 Progressive Environmental and Agricultural Technologies (PEAT). The Plantix app is used by farmers who upload photos of
 146 their crops to seek assistance in diagnosing and treating crop diseases. As part of the disease diagnosis process, PEAT uses
 147 a convolutional neural network to assign crop labels based on the submitted photos. We used labels for the years 2020 and
 148 2021 in the Indian states of Maharashtra and Uttar Pradesh (UP), where the accuracy of Plantix crop type labels exceeds 90%
 149 for most major crops. Data have been cleaned to remove location inaccuracy (keeping only submissions with GPS accuracy
 150 better than 10 m), as suggested by previous work by Wang et al. (2020). Additionally, to mitigate any bias, Plantix labels were
 151 sampled to match the proportion of government-reported crop areas by crop, as certain labels, such as those for vegetables,
 152 were more prevalent due to their susceptibility to diseases.

153 In Thailand we accessed crop type labels obtained with Google Street View (GSV) (Laguarta et al., 2023) for the year 2022.
 154 These labels were generated by combining deep learning and street view imagery over Thailand, requiring minimal manual
 155 labeling. Labels include sugarcane, cassava, maize, rice, and an “other” crop class. Labels accuracy XX To ensure the labels
 156 were representative of the landscape, they were sampled in alignment with government-reported crop areas.

157 In South Africa, independent reference points, used for validating the South African National land cover 2020 (SANLC
 158 2020) map, are provided by the Department of Forestry, Fisheries and the Environment (South Africa - DFFE).



159 **2.4.2 Raster data**

160 In Brazil and China, sugarcane masks at 30m resolution were recently published by Zheng et al. (2022a) and Zheng et al.
161 (2022b). These maps were generated using a time-weighted dynamic time warping method. In Brazil, maps are available for
162 14 states for 2016–2019, with a reported overall accuracy for the year 2018 of 91%, and user’s and producer’s accuracies
163 reaching 94% and 87%, respectively.

164 In China, maps are available for 2016–2020 for four southern provinces, which map over over 95% of the sugarcane cul-
165 tivation areas in China: Guangxi (64%), Yunnan (18%), Guangdong (12%), and Hainan (1%) provinces. The reported overall
166 accuracy for the year 2019 is 92.7%, with reported user’s and producer’s accuracies of 85.6% and 86.7%.

167 The Cropland Data Layer (CDL) (Boryan et al., 2011) produced by the United States Department of Agriculture (USDA)
168 provides yearly crop type maps across the conterminous US at 30 m spatial resolution. Maps are based on Landsat and other
169 satellite imagery using training data from the Farm Service Agency (FSA). Sugarcane plantations in the contiguous United
170 States are primarily concentrated in three states: Florida, Louisiana, and Texas. Accuracy of CDL on FSA labels are available
171 in the CDL metadata, with precision and recall for sugarcane in 2019-2022 exceeding 72%, 94% and 93% in Texas, Florida,
172 and Louisiana, respectively.

173 The South African National Land Cover 2020 (SANLC 2020), recently published by the Department of Forestry, Fisheries,
174 and the Environment (South Africa - DFFE), was generated at a 20-meter resolution utilizing S2 imagery. The overall accuracy
175 of this land cover classification is 85.5%. The accuracy for the sugarcane classes surpasses 95% for user’s accuracy and 82%
176 for producer’s accuracy.

177 **2.4.3 Government statistics**

178 The Brazilian Institute of Geography and Statistics (IBGE) (Instituto Brasileiro de Geografia e Estatística) offers comprehen-
179 sive data on various agricultural metrics, including the planted and harvested areas, production volumes, and average yields, on
180 an annual basis for agricultural commodities. In our research, we utilized the municipality-level (admin 2) data for sugarcane
181 planted and harvested areas for the latest available year, 2022.

182 In India, the Ministry Of Agriculture and Farmers Welfare releases crop production statistics (Indian Department of Agri-
183 culture) at the district level (admin 2). For our analysis, we incorporated district-level crop area statistics for the most recent
184 available year, which is the 2019–2020 growing season.

185 In China, the Statistical Yearbooks serve as annual publications providing comprehensive insights into the economic and
186 social development of each province. These publications encompass data from the previous year, offering statistics at both
187 the provincial level and the local levels of cities (level 2). For our analysis, we obtained sugarcane sown area data from the
188 Statistical Yearbook for the 2022 growing season for the four sugarcane producing provinces: Guangdong (Guangdong Provin-
189 cial Bureau of Statistics), Guangxi (Statistics Bureau of Guangxi Zhuang Autonomous Region), Yunnan (Yunnan Provincial
190 Bureau of Statistics), and Hainan (Hainan Provincial Bureau of Statistics).



191 The agricultural statistics of Thailand for the year 2022, including data on sugarcane harvested area, were sourced from the
192 relevant government authority at province level (admin 1) (Office of Agricultural Economics).

193 The district-wise statistics on crops area and production for the growing season 2021-22 in Pakistan were obtained from
194 the government of Pakistan at district level (admin 3) (Ministry of National Food Security and Research). Due to uncertainties
195 regarding district borders over time, the data were processed and aggregated at level 2 to ensure consistency and accuracy in
196 the analysis.

197 The annual agricultural statistics provided by the Government of Mexico (Agri-Food And Fisheries Information Service)
198 encompass a wide range of information, including data on planted area, harvested area, damaged area, average rural prices,
199 volume, and value of production for both cyclical and perennial crops, categorized by water modality. These reports cover all
200 32 federal entities of the country, with detailed breakdowns at the national, state, district, and municipal levels (admin 2). For
201 our analysis, we specifically extracted sugarcane area data at the municipality level for the year 2022.

202 The National Agricultural and Livestock Survey Survey (ENA) conducted in 2019 (National Administrative Statistics De-
203 partment), provides data on sugarcane planted area, production, and yield by region (admin 1) for the year 2019 in Colombia.

204 The Indonesia Central Statistics Agency (Badan Pusat Statistik (BPS)) serves as the official statistical agency of the Indone-
205 sian government, tasked with collecting, processing, analyzing, and disseminating statistical data and information throughout
206 the nation. It provides comprehensive statistics on plantation area by province (admin 1), which offers insights into the distri-
207 bution of agricultural land across different regions of Indonesia. Specifically, the dataset comprises the area of annual crops
208 such as oil Palm, coconut, rubber, coffee, cocoa, and tea, representing the planted area at the end of the year. Additionally,
209 the dataset includes information on seasonal crops like tobacco and sugarcane, with data reported as the monthly cumulative
210 harvested area. The most recent report refers to the year 2021.

211 In the United States, county-level (admin 2) statistics on sugarcane area are available from the United States Department of
212 Agriculture's National Agricultural Statistics Service (NASS) (USDA National Agricultural Statistics Service). We accessed
213 the most recent data for counties in the key sugarcane-producing states Florida, Louisiana, and Texas for the year 2018 using
214 the NASS Quickstats database.

215 Statistics on the production of agricultural commodities, encompassing cereal and broadacre crops, fruit and vegetables, and
216 livestock on Australian farms, are provided by the Australian government (Australian Bureau of Statistics). These statistics are
217 made available on a yearly basis, with the most recent data available for the 2020-2021 growing season (at Statistical Areas
218 Level 2).

219 In Guatemala, data on sugarcane production by department (admin 1) for the agricultural year 2002/2003 was obtained from
220 the IV National Agricultural Census (Guatemala National Institute of Statistics). Sugarcane accounted for 28.4% of the total area
221 cultivated with permanent and semi-permanent crops. The department of Escuintla recorded the highest sugarcane productions
222 for the census year, comprising 87.7% of the total production.

223 The Philippine Statistics Authority (PSA) (Philippine Statistics Authority) releases annual provincial statistics on Agriculture
224 and Fisheries. These statistics include the total area of sugarcane and the percent distribution of sugarcane production by
225 region. Although direct access to sugarcane area by region is not available, an approximation can be made by assuming that



226 the percentage of production falls within the same range as the percentage of area by region. The most recent year for which
227 data is available is 2021.

228 The Statistics department of South Africa (Statistics Department - South Africa) conducts the Census of Commercial Agri-
229 culture, 2017 (CoCA 2017), which publishes results at the municipal level (admin 3). The primary objective of this survey is to
230 gather financial, production, employment, and related information pertaining to the commercial agriculture industry in South
231 Africa. It is important to note that CoCA 2017 only covers enterprises registered for value-added tax (VAT). Consequently, the
232 census does not include smallholder farming. Instead, it utilizes VAT records as a sampling frame, thereby excluding entities
233 that are non-VAT registered. It is noteworthy that commercial farmers account for 80% of the country's agricultural value.

234 **3 Methods**

235 **3.1 Sugarcane phenology**

236 Sugarcane is primarily grown in tropical and sub-tropical regions of the world. It is a tall semi-perennial crop, with a growth
237 cycle lasting typically between 12 to 18 months before it is ready for harvesting. The specific duration of this cycle varies
238 depending on factors like the sugarcane variety, local climate, and geographical conditions in each region. After the first
239 harvest, sugarcane can regrow from the same root systems for multiple years (ratoon crops), resulting in subsequent yield
240 losses due to a reduction in stalk population. To ensure sustainable yields and maintain soil fertility, sugarcane areas are often
241 rotated with other crops to aid in nitrogen fixation for subsequent sugarcane growth seasons. Cultivation practices also involve
242 planting different sugarcane varieties within the same plantations to minimize susceptibility to diseases. Figure 1 provides a
243 visual example of sugarcane time series in Brazil and rotation with soybean.

244 **3.2 Area of interest**

245 We initiated our study by focusing on the main sugarcane-producing countries listed in Table 1.

246 We established a $2^\circ \times 2^\circ$ grid overlaying these countries. To reduce computation, grid cells were selected based on two
247 criteria: a cropland coverage exceeding 1%, determined using the European Space Agency (ESA) Crop Mask dataset, and
248 a sugarcane area greater than 0, derived from the Spatial Production Allocation Model (SPAM) (International Food Policy
249 Research Institute, 2019). These selected grid cells represent the regions where we aimed to predict sugarcane presence.

250 **3.3 GEDI data processing**

251 All GEDI shots from April 2019 to December 2022 over cropland pixels, passing over these $2^\circ \times 2^\circ$ grid cells, were classified
252 as either short, tall, or tree by a GEDI model trained in Di Tommaso et al. (2023). Each classification was accompanied by a
253 confidence value.

254 Prior to further analysis, the predicted shots underwent a filtering process to retain only high-quality data. Initially, shots
255 were filtered based on the quality and degrade flags provided as properties in the GEDI dataset. Additionally, predictions with



256 confidence scores lower than 0.8 were discarded. A crucial step involved filtering out shots with low view angles and those
257 over high-slope terrain, defined as areas with slopes exceeding 5° , as both factors can impact the accuracy of GEDI model
258 predictions. View angle information was retrieved from the L2B dataset, enabling the exclusion of low view angle shots.

259 Furthermore, we opted to exclude shots identified as belonging to the tree class by the GEDI model. This decision was
260 motivated by the likelihood that such shots may encompass a mixture of crops and trees within the GEDI footprint, which, at
261 a diameter of 25 meters, surpasses the size of the 10-meter S2 pixel by over four times.

262 Figure 1 shows the spatial coverage of GEDI over time and the changing proportion of tall and short labels over cropland.

263 3.4 S2 model training and classification

264 Utilizing the GEDI predictions as binary labels, we trained separate local S2 models for each grid cell and for each month
265 of the year. We opted for a random forest model for its well-documented advantages, including high accuracy, computational
266 efficiency, and smooth integration into large-scale applications within GEE. The S2 models were trained using S2 harmonics
267 coefficients as features and the GEDI predictions as labels. For each grid cell, we aggregated GEDI labels for each month across
268 different years and extracted the corresponding S2 features for the same year as the GEDI label. Subsequently, we constructed
269 pooled models for each month and generated predictions for four years, utilizing features specific to each year. This process
270 yielded 48 monthly predictions for each grid cell, where each 10 m by 10 m pixel within the crop mask was classified as either
271 short or tall.

272 In order to reduce spatial artifacts during the mosaicking of adjacent cells, we created predictions for pixels in a 0.2° buffer
273 around each cell. Subsequently, on a monthly basis, we mosaicked the overlapping predictions, selecting the predictions from
274 the cell with the higher GEDI-S2 kappa score.

275 3.5 Calibration/Sugarcane identification

276 We determined sugarcane presence by computing the frequency of tall predictions for each pixel across the 48 monthly predic-
277 tions. Pixels were classified as sugarcane if the frequency of tall predictions exceeded a certain threshold.

278 To distinguish sugarcane from other tall crops, a single threshold across all countries is not optimal, since the threshold
279 will depend on the mix of crops alongside sugarcane, the phenological characteristics of both sugarcane and other crops, and
280 agricultural management practices.

281 The selection of the threshold was guided by a calibration approach based on available *in situ* data. To determine the threshold
282 in countries where we had large number of labels of sugarcane and different crop type classes, we used point level calibration
283 and relied on the threshold that produced the highest kappa score.

$$284 \text{ Kappa score} = \frac{P_o - P_e}{1 - P_e}$$

285 where

286 – P_o is the proportion of observed agreement, i.e. the accuracy achieved by the model



287 – P_e is the proportion of agreements expected by chance

288 This methodology was applied in Brazil, India, Thailand, and South Africa, where we had many (> 600) ground samples.,
289 as well as in China and the USA where point labels were unavailable but crop type maps developed through a combination
290 of ground and satellite data were accessible. In these cases, samples were obtained by random sampling of the reference crop
291 maps.

292 In other countries with a limited availability of sugarcane labels ($n < 200$), we extracted at each location of a sugarcane
293 label the number of tall months in our map, and then calculated the 10th percentile of this value across all such locations.
294 This threshold therefore ensures that 90% of the reference sugarcane labels would be classified as sugarcane. In countries
295 where ground labels were lacking, we set the threshold equal to that of a nearby country, based on the assumption that the
296 characteristics of the sugarcane were most similar in nearby locations.

297 3.6 Validation

298 To validate our sugarcane maps, we compared them against a combination of available point samples, raster maps of crop
299 type, and reported sugarcane area of government statistics. Because of the nature of sugarcane, a semi-perennial crop, we are
300 mapping total-stable sugarcane area in the 4-year period. Although we do not expect perfect agreement against government
301 reported planted or harvested area for a single year, a comparison with government data still provides a useful assessment of
302 how well our maps capture broad spatial patterns.

303 4 Results

304 We first present the outcomes of the calibration strategy, outlining the optimal threshold for sugarcane identification based
305 on available data specific to each country. For validation purposes, we compare the results against field points and rasters
306 and assess the sugarcane area against government-reported data. These evaluations are conducted for each country using the
307 selected threshold and employing a combined ESA and GLAD crop mask. We find that combining these two maps helps cover
308 the majority of cropland in most regions while avoiding the mapping of orchards that are often included in the ESRI crop mask.
309 It's worth noting that even though results are provided for the cropland area mapped in the ESA and GLAD masks, a sugarcane
310 map is produced for the area covered by the ESRI crop mask as well, and it is made available in our dataset. Further details
311 about the data release are provided in the data availability section.

312 4.1 Calibration

313 For calibration, we employed various strategies due to the absence of in situ labels across all countries of interest. Results of
314 the calibration for countries with abundant ground samples are illustrated in Figure 3.

315 China, Thailand, and South Africa exhibit low sensitivity to the chosen threshold. In Thailand, the threshold is optimized to
316 avoid mostly confusion with cassava, a shrubby perennial that is usually 2–3 m in height. In South Africa, most of the point

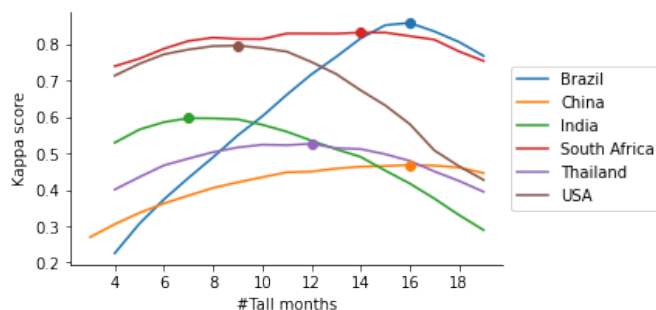


Figure 3. Identification of the threshold for classifying pixels as sugarcane based on the kappa score for countries with abundant in situ crop type labels. X-axis shows number of months (out of a total of 48) where a tall crop was present, and y-axis shows the kappa score for a model that classifies as sugarcane all pixels with at least this many months with tall crops. Dots represent the maximum kappa score value and the chosen threshold for each country. In India, 7 and 8 month thresholds were tied and we opted to use a threshold of 8 to be conservative and prioritizing higher precision in our map, avoiding the inclusion of other crops.

317 samples are sugarcane, followed by small-scale and commercial annual crops. The optimal threshold helps to avoid confusion
318 with commercial irrigated annual crops.

319 The threshold selection is critical in Brazil, mostly to avoid confusion with maize, another tall crop ranging from 1.2–4 m in
320 height.

321 India and the US exhibit moderate sensitivity and lower optimal thresholds, perhaps due to shorter sugarcane phenological
322 cycles and the absence of other crops that appear tall in sugarcane growing areas. In India, the calibration curve appears very
323 flat between 7 and 8 months. To err on the side of caution, and avoid including other crops in our sugarcane map, we chose
324 to set the threshold at 8 months. In the US, the threshold serves to avoid confusion with maize, which is present but not as
325 common as in Brazil.

326 In regions where insufficient labels were available for crop types other than sugarcane to compute a reliable kappa score, such
327 as Mexico, Australia, and the Philippines, we adopted the 10th percentile approach. Conversely, in regions where no data were
328 accessible, we determined the threshold based on the neighboring country. This last strategy was applied in Pakistan, Colombia,
329 Indonesia, and Guatemala. Results of the chosen calibration method and threshold for all the countries are summarized in Table
330 3.

331 4.2 Sugarcane Maps

332 Sugarcane maps for the main producing countries obtained applying the calibration threshold previously identified, across the
333 48 monthly predictions are shown in Figure 4.



Table 3. Summary of the thresholds used for calibrating the sugarcane maps. The threshold is expressed as the number of months over a 48 month-period. Diverse metrics and data sources have been adopted across different countries as a result of disparities of *in situ* data availability. Rows marked with N/A denote the absence of available data, and a threshold from a neighboring country was adopted. Specifically, Pakistan employed the same threshold as India, Colombia as Mexico, Indonesia as Thailand and Guatemala as Mexico. Threshold range from as low as 8 months in India, Pakistan and the Philippines, to as high as 16 months in Brazil and China. These disparities reflect differences in sugarcane phenology, management practices, and co-cultivation with other crops, tall or short.

Rank	Country	Data Source	Metric	Threshold
1	Brazil	WorldCereal	kappa	16
2	India	Plantix points	kappa	8
3	China	Raster	kappa	16
4	Thailand	GSV points	kappa	12
5	Pakistan	N/A		8
6	Mexico	WorldCereal	10th perc	14
7	Colombia	N/A		14
8	Indonesia	N/A		12
9	USA	CDL	kappa	9
10	Australia	WorldCereal	10th perc	11
11	Guatemala	N/A		14
12	Philippines	WorldCereal	10th perc	8
13	South Africa	SANLC points	kappa	14

334 4.3 Validation

335 4.3.1 Validation against field points

336 We provide a summary of point-level validation results for the sugarcane maps by country based on field-level data in Figure
337 5.

338 Performance metrics vary across countries, with F1 scores for sugarcane exceeding 0.8 for most countries. Notably, Brazil,
339 Mexico, Australia, the Philippines, and South Africa exhibit strong performance, with F1 scores higher than 0.9. However,
340 exceptions are observed in certain regions.

341 In Thailand, utilizing GSV samples yields an F1 score on sugarcane of 0.57, with precision and recall scores of 0.53 and
342 0.62, respectively. The predominant confusion is observed with the cassava class. This is not surprising given their coexistence
343 in similar geographic regions and that cassava plants can grow over 2 m. It is also common for farmers to alternate between
344 cassava and sugarcane cultivation in their fields. In contrast, performance in Thailand using WorldCereal data appears to be
345 better, but it is essential to note that cassava is not included in this dataset. WorldCereal crop classes in Thailand include rice,
346 sugarcane, and maize. Additionally the number of WorldCereal samples (75) is substantially limited compared to GSV samples
347 (~19k).

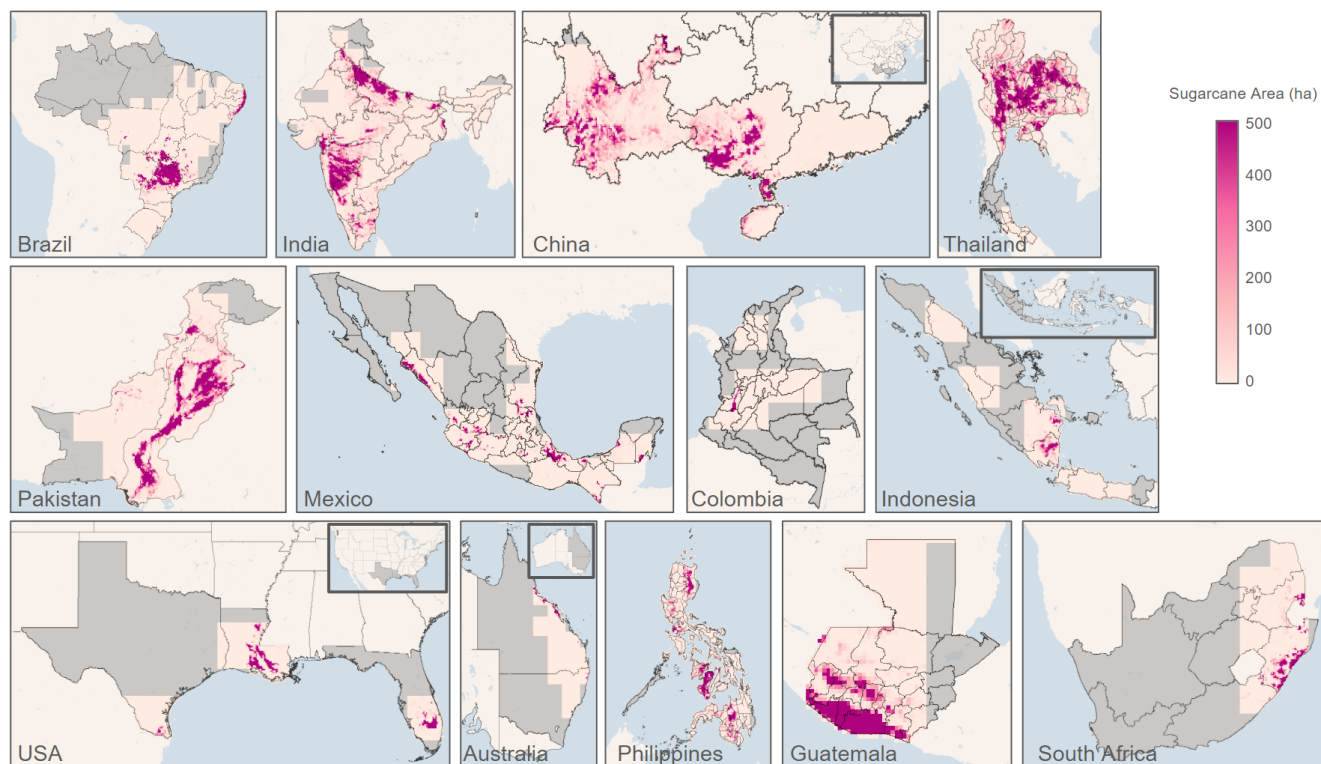


Figure 4. Sugarcane maps for top 13 producing countries (© Google Earth Engine). For visualization, the original 10 m maps were resampled at 10 km resolution and show the sugarcane area in hectares for each 10×10 km pixel (1000 ha). The area that we did not process—due to lack of cropland or sugarcane—is colored in gray. For China, Indonesia, the US, and Australia, the highlighted gray area in the inset indicates the regions for which zoom-ins are provided.

348 In India, contrasting results are observed between different datasets. For instance, using Plantix labels yields an F1 score of
349 0.67 for sugarcane, with precision and recall at 0.65 and 0.69, respectively. Notably, performance in Maharashtra (MH) lags
350 behind Uttar Pradesh (UP), with F1 scores of 0.56 and 0.7, respectively. The lower performance of MH is mostly due to low
351 precision (0.5), caused from misclassification of maize as sugarcane. Conversely, utilizing WorldCereal data in India results
352 in an F1 score of 0.82 for sugarcane, with precision and recall metrics of 1 and 0.69, respectively. This is explained by fewer
353 maize labels, with labels for the other class including mostly rice and wheat. It's worth noting in this case as well the limited
354 number of WorldCereal samples (115) in this region compared to Plantix (~37k).

355 Similarly, Pakistan, using WorldCereal labels, exhibits an F1 score of 0.6, primarily attributed to low recall (0.43).

356 4.3.2 Validation against raster datasets

357 We offer a visual comparison between reference maps and predicted sugarcane maps for regions where crop type maps are
358 available, depicted in Figure 6. In cases where multiple years of sugarcane maps were accessible but did not correspond to the

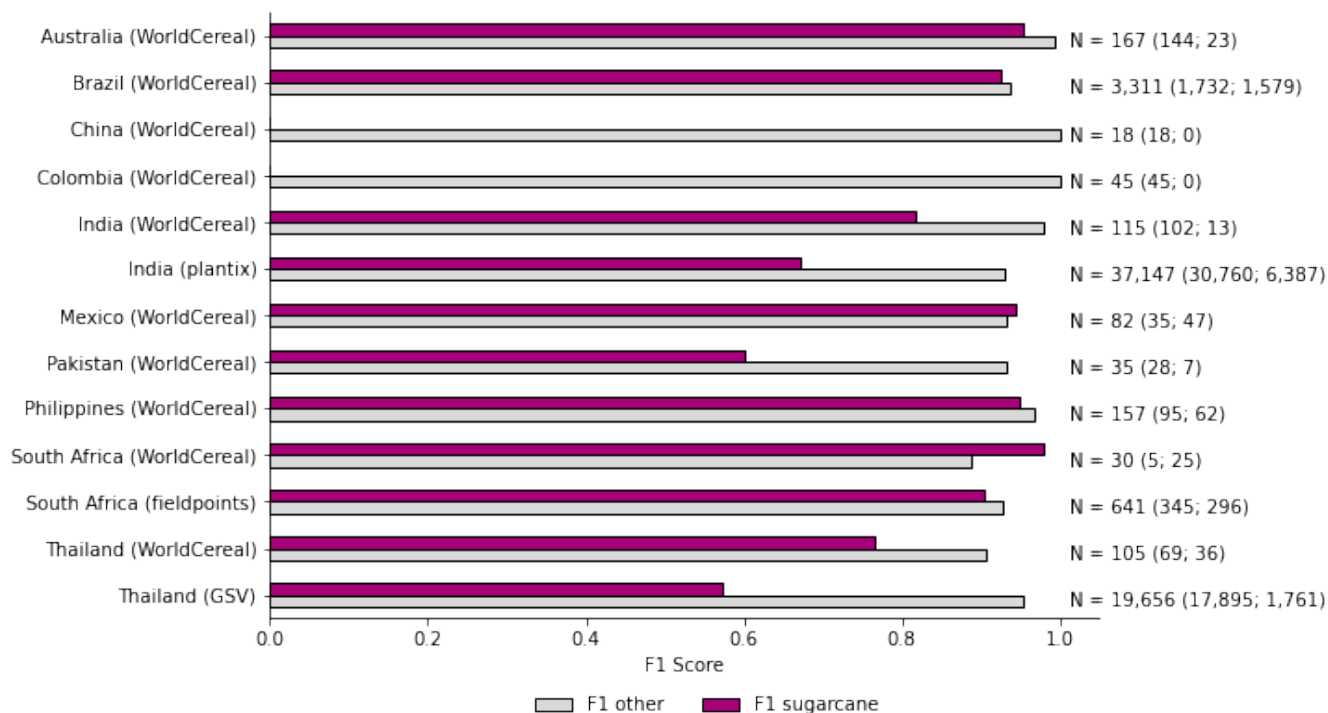


Figure 5. Results of point level validation. In parenthesis are reported the numbers of samples labeled non-sugarcane and sugarcane labels.

359 same years as our study, as in the case of Brazil and China, we utilized the two most recent years. Sugarcane was classified
360 as present in a pixel if it appeared as sugarcane at any point during these years, accounting for potential crop rotation. For the
361 US, where the Cropland Data Layer (CDL) is available annually from 2019 to 2022, we considered a pixel as sugarcane if it is
362 classified as sugarcane for at least two years out of the four.

363 To evaluate a measure of agreement between maps, we randomly sampled 10k cropland points for each state/admin1 covered
364 by the raster maps and reported F1 scores in Fig. 6. These metrics pertain to the entire mapped raster area, not just the portion
365 depicted in the zoomed-in view in the figure. Across different regions, F1 scores for sugarcane varied, ranging from 0.47 in
366 China to 0.84 in the USA.

367 In Brazil, the raster encompasses 13 states, with a relatively lower F1 score of 0.6 for sugarcane. This discrepancy is reflected
368 in the precision of 0.55 and recall of 0.66. However, in São Paulo, the F1 score improves to 0.74, characterized by higher
369 precision (0.82) and recall (0.67).

370 In China, the overall F1 score of 0.47 is derived from data spanning all four provinces. Notably, in Guangxi, the primary
371 sugarcane-producing region, the F1 score increases to 0.64, with the same precision and recall (both 0.64).

372 In the USA, precision and recall values stand at 0.85 and 0.82, respectively, indicating strong agreement between maps.

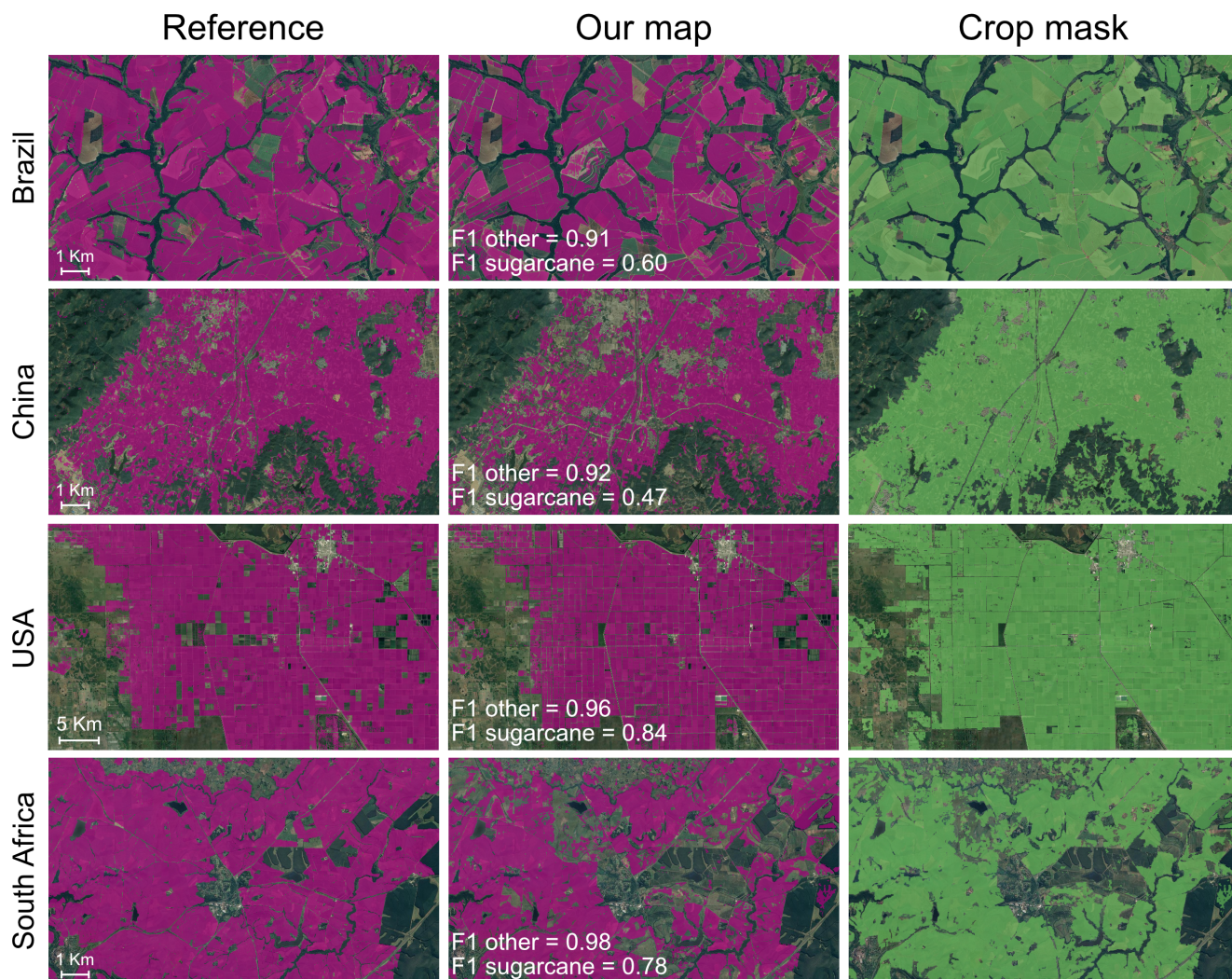


Figure 6. Comparison between our sugarcane maps and reference rasters. Maps show zoom-ins of key sugarcane-producing regions in Brazil, China, US and South Africa (© Google Earth Engine). The reported metrics pertain to the entire region covered by the reference maps, not just the illustrated portions. The absence of sugarcane in certain predicted maps for select regions can be attributed in part to the crop mask selection (ESA+GLAD), which omits certain cropped areas (e.g., South Africa).



373 Conversely, in South Africa, precision and recall are slightly lower at 0.73 and 0.84, respectively, with a portion of labels for
374 commercial annual crops misclassified as sugarcane.

375 4.3.3 Validation against government statistics

376 To evaluate the accuracy of our sugarcane maps, we conducted a comparison with government reported statistics on sugarcane
377 area. We present the results in Figure 7 at the finest available scale provided by the governments. The only exception is
378 Pakistan, where we group the data at level 2 due to uncertainties/changes of level 3 administrative division borders over time.
379 Only administrative regions fully covered by our sugarcane maps are included in these results. We find overall good agreement
380 with government statistics for the main sugarcane-producing areas. Many countries (6) exhibit an R^2 of 0.85 or higher (Brazil
381 0.92, Pakistan 0.85, USA 0.99, Australia 0.9, Guatemala 0.97, Philippines 0.85).

382 Some exceptions occur in regions where inaccurate crop masks lead to over prediction of sugarcane area. Specifically,
383 in Yunnan, China, many orchard areas are included in the crop mask, and because these are tall for the entire year tend to
384 get classified by our model as sugarcane. Moreover, regions predominantly characterized by (irrigated) maize cultivation, as
385 evident in Sinaloa, Mexico, also tend to be misclassified as sugarcane by our model, presumably because they are growing
386 maize every year of the study period. Outside of these problematic regions, the model agrees well with official statistics in each
387 country. The R^2 increases from 0.73 to 0.96 when removing Yunnan in China, and from 0.46 to 0.78 when removing Sinaloa
388 in Mexico.

389 Moving to the assessment of main sugarcane-producing states within each country, São Paulo emerges as the main con-
390 tributor to Brazil's sugarcane landscape, accounting for over half of the planted area. Here, our analysis demonstrates robust
391 agreement between predicted and government-reported sugarcane areas, with an R^2 value of 0.94 and a slope of 0.88, based
392 on 630 administrative units.

393 In India, Uttar Pradesh (UP) stands as the primary sugarcane producer, followed by Maharashtra and Karnataka, the three
394 states together contribute approximately 80% of the nation's sugarcane production. Notably, UP exhibits strong agreement
395 with government-reported data, with an R^2 value of 0.95 and a slope of 1.26. Conversely, while Maharashtra and Karnataka
396 also demonstrate a good agreement, with R^2 values of 0.79 and 0.96, respectively, the regression line slopes for both states is
397 close to 2 (2.2), suggesting that the predicted sugarcane area is more than twice the reported area.

398 In China, Guangxi has the highest cultivation land and production of sugarcane, accounting for more than 60% of the total
399 national area. We observe strong agreement with the government-reported area, with R^2 value of 0.97 and a slope of 1.

400 In Colombia, agricultural statistics are reported at the administrative level 1, known as departments. Our map provides full
401 coverage solely for the Caldas department, a minor sugarcane-producing region, with an estimated area three times smaller than
402 the reported area. It's worth noting that the primary sugarcane-producing areas, Valle de Cauca and Cauca, are only partially
403 covered by our maps. Despite this, we observe substantial agreement between the mapped areas and the government-reported
404 sugarcane area.

405 In Indonesia, statistical data on sugarcane production is available at provincial level (admin 1). However, only Jawa Barat, a
406 minor sugarcane-producing province, is fully covered by our sugarcane map, while the main sugarcane-producing provinces,

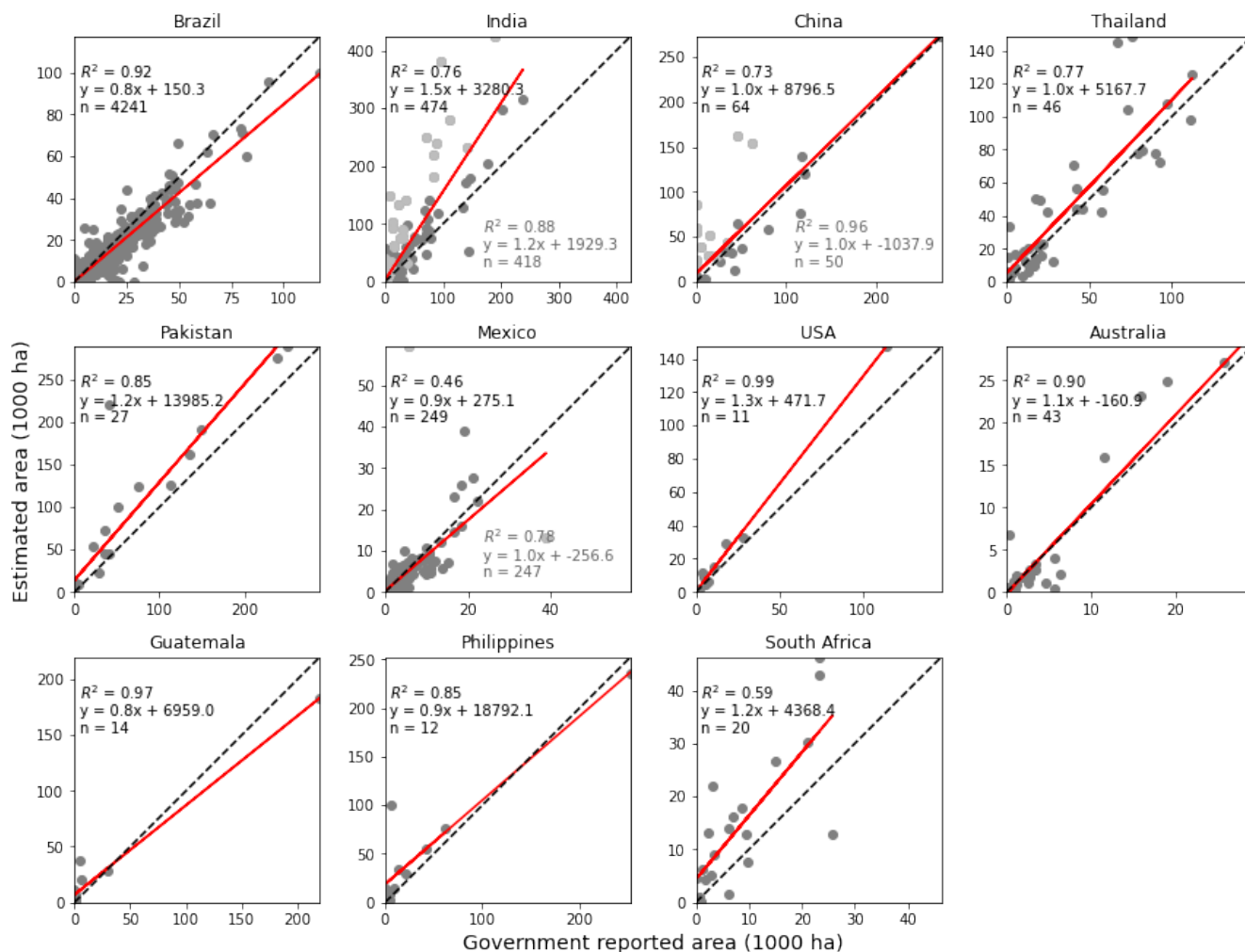


Figure 7. Comparison of the sugarcane area in our maps with government statistical data. On the top-left corner are reported the results using all data points. For some countries, on the bottom-right are reported the results removing problematic regions.

407 such as Lampung and Sumatra Selatan, have partial coverage. Despite this limitation, our analysis reveals agreement between
 408 the reported sugarcane area and the mapped areas in these provinces.

409 In US, Florida and Louisiana are the main producers, with R^2 of 1 and 0.9, respectively. In Australia, Queensland serves as
 410 the primary producer state, demonstrating an R^2 value of 0.91.

411 Regarding South Africa, the available government statistics pertain exclusively to commercial farmers, whereas our analysis
 412 includes all sugarcane fields, encompassing both commercial and smallholder operations. Despite this disparity, we report the
 413 agreement because commercial farmers contribute to over 80% of the total sugarcane production in the country. The lower R^2
 414 value may be attributed to the type of reported statistics as well as potential crop mask issues.



415 5 Discussion

416 5.1 Agreement with field data and raster

417 Synthesizing lessons from point and raster data, we find that GEDI and S2-based sugarcane mapping presents challenges,
418 particularly in regions where tall crops like cassava and maize, especially irrigated maize, coexist with sugarcane. We also
419 observe discrepancies in performance between point and raster data. In Brazil, we noticed lower performance in raster maps
420 (F1 score of 0.6) compared to WorldCereal point data (F1 score of 0.9). This discrepancy could potentially be attributed to the
421 construction of reference rasters, wherein sugarcane is defined as the union of the two most recent years, along with differences
422 in the years considered. In South Africa, it's worth noting that performance against the SANLC field points surpasses that of
423 the South Africa SANLC 2020 map. For field points, the F1 score for sugarcane is 0.9, with precision at 0.97 and recall at 0.84.
424 In contrast, the map exhibits an F1 score of 0.78, with precision and recall values of 0.73 and 0.83, respectively. In the US,
425 where we have high confidence in the CDL maps and reference map years align with our mapping period, we observe good
426 agreement with CDL sugarcane data. However, it is essential to emphasize that reference maps may not be equally reliable,
427 potentially leading to discrepancies in performance evaluation.

428 5.2 Agreement with government statistics

429 The comparisons with government statistics are complicated by several factors, including the unknown accuracy of official
430 numbers and the fact that they do not necessarily intend to reflect all of cropland area planted with sugarcane. Government
431 data often reflect sugarcane harvested area for a single year, while our mapping captures total-stable sugarcane area over a
432 four-year period. We therefore would expect our numbers to be slightly higher than government numbers, even if both datasets
433 were perfectly accurate. Despite this disparity, we generally observe favorable agreement in most regions.

434 In India, particularly in Maharashtra and Karnataka, deviations from the 1:1 line are evident, with slope values of 2.3 and
435 2.2, respectively. Notably, in Maharashtra, the mapped area (2,702,144 ha) exceeds the government-reported area (822,407
436 ha) by over 230%. However, Plantix data in Maharashtra, which was adjusted for bias in class representation as described in
437 section 2.4.1, revealed a low user's accuracy (50%). This is a warning that commission error associated with the sugarcane
438 class was problematic.

439 To address this, we employed an error-adjusted estimator of area proposed by Olofsson et al. (2013) to correct the estimated
440 sugarcane area and provide confidence intervals. Taking into account the presence of false positives, consisting of 955 instances
441 among 1,911 sugarcane labels, and false negatives, comprising 529 instances among 13,384 non-sugarcane labels, alongside a
442 proportion of area mapped as sugarcane equal to 0.15, our analysis yielded a revised estimate of sugarcane area of 1,953,625
443 ha. This revised estimate notably surpasses the reported area by approximately 140%.

444 The resulting confidence interval, computed using the method suggested by Olofsson et al. (2013), suggests that the sug-
445 arcane area estimate could range from 1,873,290 ha to 2,033,960 ha at a 95% confidence level. Despite the wide confidence
446 interval, it is still well above the government-reported area, and the gap is too large to be explained by the difference between
447 total and harvested area. We therefore suggest that the official numbers in Maharashtra are significantly underestimating the



448 actual sugarcane area. This conclusion is similar to that reached in a previous study in the Upper Bhima Basin within Maha-
449 rashtra, which concluded that actual sugarcane area may be twice as large as what is indicated in government statistics (Lee
450 et al., 2022).

451 **5.3 Future improvements**

452 A number of future directions could improve the accuracy of our maps. A key dependency in our approach is the use of
453 existing crop maps that delineate arable cropland from other land uses, including permanent tree crops. Yet we observed in
454 several regions, most notably in Southern China, that the crop mask often included areas with orchards. Because orchards are
455 tall throughout the year, removing them from the crop mask is an important need for further improvement. Likewise, in some
456 regions the crop masks we utilized miss some areas that appear in other sugarcane reference maps (e.g. in South Africa, see
457 Fig. 6). By improving the accuracy of the crop mask, more precise sugarcane maps can be generated, providing more reliable
458 information for agricultural planning and management. Implementing subnational thresholds could further refine the accuracy
459 of our estimations, considering the localized variations in sugarcane cultivation practices. Lastly, integration of other sensor
460 data, such as Sentinel-1, into our mapping framework could enhance the performance.

461 In future iterations, extending the grid to encompass more geographical areas could provide a broader perspective on sugar-
462 cane dynamics. Additionally, extending our maps back in time would allow us to examine changes over time and could offer
463 valuable insights into temporal trends.

464 **6 Conclusions**

465 In this study we have introduced a dataset of sugarcane maps for the top 13 producing countries, covering nearly 90% of global
466 production, leveraging satellite remote sensing data from GEDI and Sentinel-2 for the years 2019-2022.

467 Sugarcane cultivation stands as a vital economic activity globally, contributing significantly to food and biofuel production.
468 With a quarter of the world's ethanol production sourced from sugarcane, countries like Brazil and India are positioned to
469 substantially increase their ethanol output. However, alongside its economic benefits, sugarcane cultivation presents numerous
470 social and environmental challenges, including water scarcity, soil pollution, and labor exploitation. Despite its pivotal role in
471 economies worldwide, reliable information on sugarcane cultivation remains scarce.

472 Our methodology overcomes limitations of traditional ground-based data collection, offering a scalable approach to mapping
473 sugarcane canopies globally. Through comparisons with field data, pre-existing maps, and government statistics, we have
474 demonstrated the accuracy and reliability of our maps.

475 However, challenges persist, particularly in regions where tall crops like cassava and maize coexist with sugarcane. Addi-
476 tionally, our approach's dependency on existing crop maps to delineate arable cropland from other land uses presents another
477 hurdle. These challenges underscore the necessity for ongoing refinement of our mapping techniques.

478 The final maps should be useful in studying the socio-economic and environmental impacts of sugarcane cultivation and
479 producing maps of related outcomes such as sugarcane yields.



480 **Data availability statement**

481 The final output of our study comprises the frequency of tall mappings for each 10 by 10 m pixel in the combined crop mask
482 (union of ESA, ESARI and GLAD), alongside the sugarcane maps for each country obtained applying the calibration threshold
483 and the crop masks used. Results were provided for each region using the calibration threshold and masking maps using the
484 union of the ESA and GLAD crop masks. However, with the dataset provided, users have the flexibility to use a region-
485 specific crop mask and their own region-specific thresholds if they possess additional insight or calibration data, allowing for
486 customization of the sugarcane mapping process.

487 The dataset is available on Google Earth Engine at https://code.earthengine.google.com/?asset=projects/lobell-lab/gedi_sugarcane/maps/imgColl_10m_ESAESRIGLAD and for download from Zenodo at <https://doi.org/10.5281/zenodo.10871164>
488 (Di Tommaso et al., 2024)
489

490 **Author contributions**

491 SD, SW and DL designed the research. SD developed the model code and performed the analysis. SD prepared the manuscript
492 with contributions from all co-authors.

493 **Competing interests**

494 The authors declare that they have no conflict of interest.

495 **Acknowledgements**

496 We thank Yuan Wenping for sharing the China sugarcane map, and the Google Earth Engine team for making large-scale
497 computational resources available to researchers.

498 This work was supported by the NASA Harvest Consortium (NASA Applied Sciences Grant No. 80NSSC17K0652, sub-
499 award 54308-Z6059203 to DBL).



500 References

- 501 Agri-Food And Fisheries Information Service: Mexico Statistical Yearbook of Agricultural Production, Available online: <https://www.gob.mx/siap> (accessed: February 8, 2024).
- 502
- 503 Agriculture and Agri-Food Canada: Annual Crop Inventory, Available online: <https://open.canada.ca/data/en/dataset/ba2645d5-4458-414d-b196-6303ac06c1c9> (accessed: February 26, 2024).
- 504
- 505 Allan, H. L., van de Merwe, J. P., Finlayson, K. A., O'Brien, J. W., Mueller, J. F., and Leusch, F. D. L.: Analysis of sugar-
506 cane herbicides in marine turtle nesting areas and assessment of risk using *in vitro* toxicity assays, *Chemosphere*, 185, 656–664,
507 <https://doi.org/10.1016/j.chemosphere.2017.07.029>, 2017.
- 508 Australian Bureau of Statistics: Agricultural Commodities, Australia, Available online: <https://www.abs.gov.au> (accessed: February 8, 2024).
- 509 Badan Pusat Statistik (BPS): Indonesia Plantation Area by Province 2021, Available online: <https://www.bps.go.id/> (accessed: February 15,
510 2024).
- 511 Boryan, C., Yang, Z., Mueller, R., and Craig, M.: Monitoring US agriculture: the US Department of Agriculture, National Agricultural
512 Statistics Service, Cropland Data Layer Program, Geocarto International, 26, 341–358, <https://doi.org/10.1080/10106049.2011.562309>,
513 2011.
- 514 Di Tommaso, S., Wang, S., and Lobell, D. B.: Combining GEDI and Sentinel-2 for wall-to-wall mapping of tall and short crops, *Environ-
515 mental Research Letters*, 16, 125 002, 2021.
- 516 Di Tommaso, S., Wang, S., Vajipey, V., Gorelick, N., Strey, R., and Lobell, D. B.: Annual Field-Scale Maps of Tall and Short Crops at
517 the Global Scale Using GEDI and Sentinel-2, *Remote Sensing*, 15, 4123, <https://doi.org/10.3390/rs15174123>, number: 17 Publisher:
518 Multidisciplinary Digital Publishing Institute, 2023.
- 519 Di Tommaso, S., Wang, S., Strey, R., and Lobell, D. B.: Mapping Sugarcane Globally at 10 m Resolution Using GEDI and Sentinel-2,
520 <https://doi.org/10.5281/zenodo.10871164>, 2024.
- 521 Dubayah, R., Blair, J. B., Goetz, S., Fatoyinbo, L., Hansen, M., Healey, S., Hofton, M., Hurtt, G., Kellner, J., Luthcke, S., Armston, J.,
522 Tang, H., Duncanson, L., Hancock, S., Jantz, P., Marselis, S., Patterson, P. L., Qi, W., and Silva, C.: The Global Ecosystem Dynamics
523 Investigation: High-resolution laser ranging of the Earth's forests and topography, *Science of Remote Sensing*, 1, 100 002, 2020.
- 524 El Chami, D., Daccache, A., and El Moujabber, M.: What are the impacts of sugarcane production on ecosystem services and human well-
525 being? A review, *Annals of Agricultural Sciences*, 65, 188–199, <https://doi.org/10.1016/j.aoas.2020.10.001>, 2020.
- 526 Food and Agriculture Organization's Statistical Database (FAOSTAT): Country-Wise Sugarcane Area and Production Data, 2022, Available
527 online: <https://www.fao.org/faostat/en/#data/QCL> (accessed: February 16, 2024).
- 528 Gitelson, A. A., Vina, A., Ciganda, V., Rundquist, D. C., and Arkebauer, T. J.: Remote estimation of canopy chlorophyll content in crops,
529 *Geophysical Research Letters*, 32, <https://doi.org/10.1029/2005GL022688>, 2005.
- 530 Gorelick, N., Hancher, M., Dixon, M., Ilyushchenko, S., Thau, D., and Moore, R.: Google Earth Engine: Planetary-scale geospatial analysis
531 for everyone, *Remote sensing of Environment*, 202, 18–27, 2017.
- 532 Guangdong Provincial Bureau of Statistics: Guangdong Statistical Yearbook, Available online: <http://stats.gd.gov.cn/gdtjnj/index.html> (ac-
533 cessed: February 8, 2024).
- 534 Guatemala Nationl Institue of Statistics: National Agricultural Census 2002-2003 - Volume III, Available online: <https://www.ine.gob.gt/>
535 (accessed: February 16, 2024).



- 536 Hainan Provincial Bureau of Statistics: Hainan Statistical Yearbook, Available online: <https://stats.hainan.gov.cn/> (accessed: February 8,
537 2024).
- 538 Healey, S. P., Yang, Z., Gorelick, N., and Ilyushchenko, S.: Highly local model calibration with a new GEDI LiDAR asset on Google Earth
539 Engine reduces landsat forest height signal saturation, *Remote Sensing*, 12, 2840, 2020.
- 540 Indian Department of Agriculture: Ministry of Agriculture and Farmers' Welfare, Crop Production Statistics Information System, Available
541 online: <https://aps.dac.gov.in/APY/Index.htm> (accessed: August 8, 2023).
- 542 Instituto Brasileiro de Geografia e Estatística: IBGE, Available online: <https://www.ibge.gov.br/> (accessed: November 15, 2023).
- 543 International Food Policy Research Institute: Global Spatially-Disaggregated Crop Production Statistics Data for 2010 Version 2.0,
544 <https://doi.org/10.7910/DVN/PRFF8V>, 2019.
- 545 Jenkins, B., Baptista, P., and Porth, M.: Collaborating for Change in Sugar Production: Building blocks for sustainability at scale, 2015.
- 546 Karra, K., Kontgis, C., Statman-Weil, Z., Mazzariello, J. C., Mathis, M., and Brumby, S. P.: Global land use/land cover with Sentinel 2 and
547 deep learning, in: 2021 IEEE international geoscience and remote sensing symposium IGARSS, pp. 4704–4707, IEEE, 2021.
- 548 Kerner, H., Nakalembe, C., Yang, A., Zvonkov, I., McWeeny, R., Tseng, G., and Becker-Reshef, I.: How accurate are existing land cover
549 maps for agriculture in Sub-Saharan Africa?, 2023.
- 550 Laguarda, J., Friedel, T., and Wang, S.: Combining deep learning and street view imagery to map smallholder crop types, [http://arxiv.org/abs/](http://arxiv.org/abs/2309.05930)
551 2309.05930, arXiv:2309.05930 [cs], 2023.
- 552 Lee, J. Y., Naylor, R. L., Figueroa, A. J., and Gorelick, S. M.: Water-food-energy challenges in India: political economy of the sugar industry,
553 *Environmental Research Letters*, 15, 084 020, <https://doi.org/10.1088/1748-9326/ab9925>, publisher: IOP Publishing, 2020.
- 554 Lee, J. Y., Wang, S., Figueroa, A. J., Strey, R., Lobell, D. B., Naylor, R. L., and Gorelick, S. M.: Mapping Sugarcane in Central India with
555 Smartphone Crowdsourcing, *Remote Sensing*, 14, 703, 2022.
- 556 Lesiv, M., Bilous, A., Bayas, J. C. L., Karanam, S., and Fritz, S.: Global Crop Type Validation Data Set for ESA WorldCereal System,
557 <https://doi.org/10.5281/zenodo.7825628>, 2023.
- 558 Ministry of National Food Security and Research: Pakistan Government statistics, Available online: <https://mnfsr.gov.pk> (accessed: Septem-
559 ber 28, 2023).
- 560 National Administrative Statistics Department: DANE National agricultural survey, Available online: <https://www.dane.gov.co> (accessed:
561 February 14, 2024).
- 562 OECD: Agricultural Policy Monitoring and Evaluation 2023, <https://doi.org/10.1787/b14de474-en>, 2023.
- 563 OECD, Food, and of the United Nations, A. O.: OECD-FAO Agricultural Outlook 2023-2032, <https://doi.org/10.1787/08801ab7-en>, 2023.
- 564 Office of Agricultural Economics: Thailand Statistical Yearbook, Available online: <https://www.oae.go.th/> (accessed: January 18, 2024).
- 565 Olofsson, P., Foody, G. M., Stehman, S. V., and Woodcock, C. E.: Making better use of accuracy data in land change studies: Es-
566 timating accuracy and area and quantifying uncertainty using stratified estimation, *Remote Sensing of Environment*, 129, 122–131,
567 <https://doi.org/10.1016/j.rse.2012.10.031>, 2013.
- 568 Philippine Statistics Authority: Philippines Selected Statistics on Agriculture and Fisheries, Available online: <https://psa.gov.ph/> (accessed:
569 February 13, 2024).
- 570 Potapov, P., Turubanova, S., Hansen, M. C., Tyukavina, A., Zalles, V., Khan, A., Song, X.-P., Pickens, A., Shen, Q., and Cortez, J.:
571 Global maps of cropland extent and change show accelerated cropland expansion in the twenty-first century, *Nature Food*, 3, 19–28,
572 <https://doi.org/10.1038/s43016-021-00429-z>, number: 1 Publisher: Nature Publishing Group, 2022.



- 573 Roy, S., Swetnam, T., Robitaille, A., Trochim, E., and Pasquarella, V.: samapriya/awesome-gee-community-datasets: Community Catalog
574 (1.0.1). Available at <https://doi.org/10.5281/zenodo.7271726> (accessed 2024-02-02), 2024.
- 575 South Africa - DFFE: South African National Landcover Data (SANLC) 2020, Available online: [https://egis.environment.gov.za/gis_data_](https://egis.environment.gov.za/gis_data_downloads)
576 [downloads](https://egis.environment.gov.za/gis_data_downloads) (accessed: August 1, 2023).
- 577 Statistics Bureau of Guangxi Zhuang Autonomous Region: Guangxi Statistical Yearbook, Available online: <http://tjj.gxzf.gov.cn/> (accessed:
578 February 8, 2024).
- 579 Statistics Department - South Africa: Census of commercial agriculture, 2017, Available online: <https://www.statssa.gov.za/> (accessed: Febru-
580 ary 16, 2024).
- 581 USDA National Agricultural Statistics Service: NASS Quick Stats API, Available online: <https://www.nass.usda.gov/> (accessed: February
582 1, 2024).
- 583 Wang, S., Di Tommaso, S., Faulkner, J., Friedel, T., Kennepohl, A., Strey, R., and Lobell, D. B.: Mapping Crop Types in Southeast India
584 with Smartphone Crowdsourcing and Deep Learning, *Remote Sensing*, 12, 2020.
- 585 Yunnan Provincial Bureau of Statistics: Yunnan Statistical Yearbook, Available online: <https://stats.yn.gov.cn/> (accessed: February 8, 2024).
- 586 Zanaga, D., Van De Kerchove, R., De Keersmaecker, W., Souverijns, N., Brockmann, C., Quast, R., Wevers, J., Grosu, A., Paccini, A.,
587 Vergnaud, S., et al.: ESA WorldCover 10 m 2020 v100, Zenodo: Geneve, Switzerland, 2021.
- 588 Zheng, Y., dos Santos Luciano, A. C., Dong, J., and Yuan, W.: High-resolution map of sugarcane cultivation in Brazil using a phenology-
589 based method, *Earth System Science Data*, 14, 2065–2080, <https://doi.org/10.5194/essd-14-2065-2022>, 2022a.
- 590 Zheng, Y., Li, Z., Pan, B., Lin, S., Dong, J., Li, X., and Yuan, W.: Development of a Phenology-Based Method for Identifying Sugarcane Plan-
591 tation Areas in China Using High-Resolution Satellite Datasets, *Remote Sensing*, 14, 1274, <https://doi.org/10.3390/rs14051274>, number:
592 5 Publisher: Multidisciplinary Digital Publishing Institute, 2022b.